Limnol. Oceanogr., 53(1), 2008, 255–265

Contrasting photoacclimation costs in ecotypes of the marine eukaryotic picoplankter *Ostreococcus*

Christophe Six and Zoe V. Finkel
Mount Allison University, 63B York Street, Sackville, New Brunswick, Canada

Francisco Rodriguez,[1] *Dominique Marie, and Frédéric Partensky*
Station Biologique, UMR 7144 CNRS et Université Pierre et Marie Curie, B.P. 74, 29682 Roscoff cedex, France

Douglas A. Campbell[2]
Mount Allison University, 63B York Street, Sackville, New Brunswick, Canada

Abstract

Ostreococcus, the smallest known marine picoeukaryote, includes low- and high-light ecotypes. To determine the basis for niche partitioning between *Ostreococcus* sp. RCC809, isolated from the bottom of the tropical Atlantic euphotic zone, and the lagoon strain *Ostreococcus tauri*, we studied their photophysiologies under growth irradiances from 15 μmol photons m^{-2} s^{-1} to 800 μmol photons m^{-2} s^{-1} with a common nutrient replete regime. With increasing growth irradiance, both strains down-regulated cellular chlorophyll *a* and chlorophyll *b* (Chl *a* and Chl *b*) content, increased xanthophyll de-epoxidation correlated with nonphotochemical excitation quenching, and accumulated lutein. Ribulose-1,5-bisphosphate carboxylase/oxygenase content remained fairly stable. Under low-growth irradiances of 15–80 μmol photons m^{-2} s^{-1}, *O.* sp. RCC809 had equivalent or slightly higher growth rates, lower Chl *a*, a higher Chl *b* : Chl *a* ratio, and a larger photosystem II (PSII) antenna than *O. tauri*. *O. tauri* was more phenotypically plastic in response to growth irradiance, with a larger dynamic range in growth rate, Chl *a*, photosystem cell content, and cellular absorption cross-section of PSII. Estimating the amino acid and nitrogen costs for photoacclimation showed that the deep-sea oceanic *O.* sp. RCC809 relies largely on lower nitrogen cost changes in PSII antenna size to achieve a limited range of σ-type light acclimation. *O.* sp. RCC809, however, suffers photoinhibition under higher light. This limited capacity for photoacclimation is compatible with the stable low-light and nutrient conditions at the base of the euphotic layer of the tropical Atlantic Ocean. In the more variable, high-nutrient, lagoon environment, *O. tauri* can afford to use a higher cost n-type acclimation of photosystem contents to exploit a wider range of light.

Picophytoplankton (cells <2 μm in diameter) are important contributors to marine primary productivity, biogeochemical cycling, and the function of marine food webs (Partensky et al. 1999; Worden et al. 2004). The photosynthetic prokaryotes *Synechococcus* and *Prochlorococcus* often dominate the picophytoplankton biomass, and have often been used as type organisms to characterize the physiological responses of picophytoplankton to support ecological or biogeochemical models (Gregg et al. 2003; Anderson 2005). Distinct ecotypes of *Prochlorococcus* have been isolated from different marine ecological niches (Partensky et al. 1999). Surface- and low-light–adapted *Prochlorococcus* strains show distinct nutrient uptake capacities (Moore et al. 2002) and photophysiological features (Moore et al. 1995). Specifically, the low-light *Prochlorococcus* ecotypes possess more genes which encode the Prochlorophyte chlorophyll-binding proteins (Pcb) than surface ecotypes, encoding a much larger photosynthetic antenna, organized in large rings around their reaction centers (Bibby et al. 2003).

Although a considerable fraction of marine picophytoplankton is prokaryotic, picoeukaryotic phytoplankton can account for a large fraction of the biomass of the euphotic zone (Worden et al. 2004) and are widely represented in marine waters. The green algal class Prasinophyceae (Chlorophyta) is one of the more abundant marine photosynthetic picoeukaryotic groups (Not et al. 2004; Worden et al. 2004). The Prasinophyceae are a primitive group branching at the base of the extant green lineage and are often minute in cell size and fairly simple in morphology, as exemplified by *Ostreococcus tauri*, the smallest known photosynthetic eukaryote. *O. tauri* is

[1] Present address: Centro Oceanográfico de Canarias (IEO), Ctra. San Andrés s/n, 38180, Sta. Cruz de Tenerife, Spain.

[2] Corresponding author (dcampbell@mta.ca; phone: 506 364 2610; fax: 506 364 2505).

Acknowledgments

We thank the Natural Sciences and Engineering Research Council of Canada for operating funding (ZVF, DAC), the Canada Foundation for Innovation for infrastructure (ZVF, DAC), and the Canada Research Chairs for personnel funding (DAC). F. Rodriguez was supported by a postdoctoral fellowship from Fundación Caixanova (Spain). The Roscoff group acknowledges the programs Biosope (Biogeochemistry & Optics South Pacific Experiment, Centre National pour la Recherche Scientifique—Institut National des Sciences de l'Univers), and PicoDiv (Picoplankton Diversity, EVK3-CT-1999-00021). We thank C. M. Brown for useful discussion and comments on the manuscript. We thank C. Fuller for the Carbon, Hydrogen, Nitrogen analyses and A. Cockshutt for advice on the quantitative immunoblotting procedure. AgriSera kindly provided global antibodies; Environmental Proteomics provided protein quantitation standards. We thank the reviewers for their helpful comments.

a naked, ~0.9-μm, coccoid cell with a single chloroplast, mitochondrion, and starch grain (Chrétiennot-Dinet et al. 1995) and a small, 12.5-Mbp genome which has recently been sequenced (Derelle et al. 2006). *Ostreococcus* strains have been isolated from various oceanic locations and depths (Guillou et al. 2004; Worden et al. 2004).

Ostreococcus is a good model system from an ecological and physiological standpoint because it is the smallest known picoeukaryote, and it is a good model system from an evolutionary standpoint because it is a primitive or ancestral chlorophyte. Photosynthetic organisms can acclimate their light capture relative to their metabolic requirements by tuning the size of the light harvesting complexes (LHCs) serving the reaction centers, or their photosystem content, or their cellular content of other protein complexes such as ribulose-1,5-bisphosphate carboxylase/oxygenase (RuBisCO). The LHC in photosystem II (PSII), or LHCII, is also important in the regulated dissipation of excess excitation energy. In chlorophytes, this nonphotochemical quenching (NPQ) depends largely upon the xanthophyll cycle operation and the PsbS protein, a member of the chorophyll *a*:chlorophyll *b*–binding (Chl *a*:Chl *b*–binding) protein family (Li et al. 2000; Horton and Ruban 2005) The structural and enzymatic bases of xanthophyll cycle operation have been established for the Prasinophyceae *Mantoniella squamata* (Goss 2003), but very little is known about the comparative capacities for photon dissipation and photoacclimation among Prasinophyceae.

Interestingly, a recent study has shown that the *Ostreococcus* genus includes distinct genotypes adapted to either high- or low-light environments, giving the first evidence of ecotypic differentiation of light adaptation in eukaryotic picophytoplankton (Rodríguez et al. 2005). The *Ostreococcus* strains currently cultured are dispersed in four distinct phylogenetic clades based on 18S ribosomal ribonucleic acid (rRNA) and intergenic transcribed spacer (ITS) phylogenies (Guillou et al. 2004; Rodríguez et al. 2005), and this separation is in agreement with their photophysiological features and ecological origins. For instance, strains belonging to clade B, which have been isolated at the bottom of the euphotic zone, cannot grow under high light and contain the unusual chlorophyll CS-170 (Rodríguez et al. 2005).

The discovery of light–shade ecotypic differentiation in picoeukaryotic phytoplankton, similar to that previously reported in *Prochlorococcus*, raises questions on how their distinct genotypes result in niche partitioning. We quantitatively compared the photophysiologies of two *Ostreococcus* ecotypes isolated from contrasting ecological niches; we grew the tropical strain *Ostreococcus*. sp. RCC809 (isolated at 105 m depth) and the lagoon strain *O. tauri* under a range of irradiance. We present data revealing fundamental differences in the mechanisms and capacities for light acclimation between the two strains and interpret our results in the context of photoacclimation strategies and adaptation to the light and nutrient regimes of their respective ecological niches.

Materials and methods

Culture conditions and growth rates—O. tauri (strain OTH95) and *O.* sp. RCC809 (clone derived from strain RCC141; Rodríguez et al. 2005) were maintained in polystyrene flasks (Corning) containing K medium (Keller et al. 1987) at 22 ± 1°C under continuous white light provided by fluorescent tubes (daylight, Sylvania). Origins of the strains are detailed in Rodríguez et al. (2005). Light experiments were conducted over irradiances ranging from 5 μmol photons m^{-2} s^{-1} to 800 μmol photons m^{-2} s^{-1} adjusted with neutral density filters (LEE Filters, Panavision), as described by Six et al. (2004) and Rodríguez et al. (2005). The cultures were acclimated to the different light levels for at least 1 month before any experimental measurement. Each of the following measurements was carried out on three to four culture replicates.

Cell concentrations of exponential phase cultures grown under different growth irradiances were assessed on aliquots fixed in 0.2% glutaraldehyde (Sigma Aldrich), snap frozen in liquid nitrogen (BOC Gases), and stored at −80°C. Cell concentrations were determined using a flow cytometer (FACSort, Becton Dickinson) for which laser emission was set at 488 nm, or by visual enumeration on a hemacytometer slide (Fisher). Growth rates (μ, in day^{-1}) were computed as the slope of an ln(Nt)-versus-time plot, where Nt was cell number at time t.

Pigment analyses—Chl *a* and Chl *b* concentrations in the cultures were determined by absorption after extraction in 80% cold acetone saturated with magnesium carbonate. All manipulations were carried out on ice under subdued light. Optical densities were corrected for background with an 80% acetone blank within a spectrophotometer (UV-1700, Shimadzu) and the Chl concentrations were calculated following Porra (2002).

Pigment compositions were determined by high-performance liquid chromatography (HPLC) as described by Six et al. (2005). Briefly, about 30 mL of culture were filtered on glass-fiber filter (GFF 25 mm, Whatman), snap frozen and stored at −80°C until analysis. Pigments were extracted by crushing the filter in 1 mL of 95% cold methanol followed by 1 h of incubation at −20°C in darkness. A volume of 100 μL of filtered pigment extract was injected into an HPLC system (HP1100, Hewlett Packard) equipped with a Waters Symmetry C_8 column (150 × 4.6 mm, 3.5-μm particle size and 150 × 7.8 mm, 7-μm particle size, respectively), a diode array detector and a quaternary pump system (HP1100, Hewlett Packard). Chlorophylls and carotenoids were detected by their absorbance at 440 nm and identified using diode array spectroscopy (Hewlett Packard). The identification and titration of the pigments were carried out using classical extinction coefficients and standard curves generated using known concentrations of pigment standards (Jeffrey et al. 1997; Repeta and Bjørnland 1997). The de-epoxidation state of the xanthophyll cycle (DES) including the xanthophylls violaxanthin (Vio), antheraxanthin (Ant), and zeaxanthin (Zea) was calculated using DES = (Zea + 0.5 Ant):(Vio + Ant + Zea) (Munne-Bosch and Cela 2006).

Determination of photosynthetic parameters—Light-response curves of photosynthetic parameters were measured using a Xenon-PAM fluorometer (Walz) connected to

a temperature-controlled cuvette holder (Walz). The sample was dark-adapted for 10 min, and the modulated measuring light (4 Hz; Walz) was turned on. A saturating white-light pulse (4,000 μmol photons m^{-2} s^{-1}, 500 ms) was triggered, and the PSII fluorescence yield in the dark, $F_V : F_M$, was calculated using

$$F_V : F_M = (F_M - F_0) : F_M \quad (1)$$

where F_0 and F_M were the basal and maximal fluorescence in dark adapted samples, respectively. Culture samples were then submitted to a series of increasingly instantaneous irradiances of white light provided by a halogen lamp (Walz) in steps of 2 min from dark to ~1,000 μmol photons m^{-2} s^{-1}. After each illumination step a saturating white-light pulse was triggered in order to determine the maximal fluorescence in the light-adapted samples (F'_M), followed by a brief dark period in order to determine the basal fluorescence level in the light-adapted sample (F'_0). The photochemical quenching (Q_P) and NPQ parameters were calculated using

$$Q_P = (F'_M - F_S) : (F'_M - F'_0) \quad (2)$$

$$NPQ = (F_M - F'_M) : F'_M \quad (3)$$

where F_S was the fluorescence level just prior to the flash.

The functional absorption cross-section of PSII (σ_{PSII}, in nm^2 $PSII^{-1}$) was determined using a Fluorescence Induction and Relaxation (FIRe) fluorimeter (Satlantic). A 2-mL culture was dark-adapted for 10 min and a 100-μs single-turnover flash was applied by a blue LED (455 ± 20 nm; Walz) in order to cumulatively saturate PSII and drive fluorescence induction to the maximal fluorescence F_M. The fluorescence rise was analyzed using FIRePro software (Satlantic) and σ_{PSII} was estimated (Gorbunov et al. 1999). The absolute σ values were determined according to the calibration factor provided by Satlantic. To determine σ_{PSII} under actinic light, the sample was illuminated for 2 min at growth irradiance with blue light provided by a second set of actinic blue LEDs (455 nm; Satlantic). Thus, σ_{PSII} was determined on the remaining open PSII reaction centers at the end of each irradiance step. In addition, the cellular PSII absorption cross-section ($\sigma_{PSII\text{-}cell}$, in nm^2 $cell^{-1}$) was estimated using

$$\sigma_{PSIIcell} = [PSII\ cell^{-1}] \times \sigma_{PSII} \quad (4)$$

where [PSII $cell^{-1}$] was the cellular content of PSII (in PsbA $cell^{-1}$, below) and σ_{PSII} was the PSII absorption cross-section (nm^2 $PSII^{-1}$, above) measured in the dark.

The electron transport rate, expressed in e^- Chl a^{-1} s^{-1}, was estimated using the formula of Mackenzie et al. (2005):

$$\text{electron transport rate} = [PSII\ Chl^{-1}] \times \sigma_{PSII} \times Q_P \times I \quad (5)$$

where [PSII Chl^{-1}] was the PSII content per Chl *a*; σ_{PSII} was the absorption cross-section in nm^2 per PSII; Q_P was the photochemical fluorescence quenching reflecting the proportion of open PSII, and I was the irradiance in photons nm^{-2} s^{-1}.

Quantitation of proteins by immunoblotting—Exponentially growing cells were harvested on a 25-mm glass-fibre filter (GFF, Whatman), snap frozen in liquid nitrogen, and stored at −80°C until protein extraction. The filters were thawed in 400 μL of extraction buffer containing 140 mmol L^{-1} tris(hydroxymethyl)aminomethane (Trizma base; Sigma-Aldrich), 105 mmol L^{-1} 2-amino-2-(hydroxymethyl)-1,3-propanediol, hydrochloride (Tris-HCl; Sigma-Aldrich), 2% lithium dodecyl sulfate (LDS; Sigma-Aldrich), 10% (w : vol) glycerol, 0.5 mmol L^{-1} ethylenediaminetetraacetic acid (EDTA; Sigma-Aldrich), and 0.1 mg mL^{-1} PefaBloc SC (4-[2-aminoethyl]-benzenesulfonyl fluoride hydrochloride) protease inhibitor (Roche). The proteins were extracted in this buffer by two rounds of flash freezing in liquid nitrogen and thawing by sonication. All manipulations were carried out under subdued light on ice. The samples were then centrifuged at 10,000 × *g* for 10 min to remove filter debris. The supernatant was collected, and the total protein concentration was determined using the modified Lowry RC/DC protein assay kit (Biorad).

For each sample, a volume containing 5 μg total protein was mixed with the extraction buffer in order to obtain a 10-μL volume, and 2 μL of dithiotreitol (DTT; 0.5 mmol L^{-1}; Eppendorf) and 1 μL of blue dye (NuPAGE, Invitrogen) were added. Samples were heated for 5 min at 70°C, centrifuged for 5 min at 10,000 × g at room temperature, and loaded on a 4–12% acrylamide precast NuPAGE mini-gel (Invitrogen). Along with the samples, four loads of protein standards of either PsbA, PsaC, or RbcL (Agrisera) of known concentration were loaded in order to establish a standard curve. Electrophoresis took place for 40 min at 200 V in a 2-[N-morpholino]ethanesulfonic acid (MES)-sodium dodecyl sulfate (SDS) running buffer (Invitrogen). Proteins were then transferred on a methanol-prehydrated polyvinylidene difluoride (PVDF) membrane (Sigma-Aldrich) using a liquid transfer system (Invitrogen) for 70 min at 30 V for two mini-gels, in a transfer buffer pH 7.2 (1.25 mmol L^{-1} N,N-bis(2-hydroxyethyl) glycine (Bicine), 1.25 mmol L^{-1} Bis(2-hydroxyethyl)iminotris(hydroxymethyl)methane (Bis-tris), 0.05 mmol L^{-1} EDTA, 5 mmol L^{-1} DTT, 2.5 μmol L^{-1} chlorobutanol, and 10% methanol). Following the protein transfer, the membrane was immediately immersed in Tween 20-tris-buffered saline (Tween-TBS (Sigma-Aldrich)) buffer pH 7.6 (0.1% Tween 20, 350 mmol L^{-1} sodium chloride, 20 mmol L^{-1} Trizma base) containing 2% (w : vol) blocking agent (Amersham Biosciences) overnight at 4°C.

Primary antibodies directed against PsbA (D1 PSII core subunit; Agrisera), PsaC (photosystem I [PSI] core subunit; Agrisera), Lhca2 (PSI antenna protein; Agrisera), Lhcp (Prasinophyte-specific PSII antenna protein; courtesy of E. Rhiel, Philipps-Universität, Marburg, Germany) or RbcL (large RuBisCO subunit; Agrisera) were diluted at 1 : 50,000 in Tween-TBS in the presence of 2% blocking agent and the membrane was soaked in this solution for 1 h with slow agitation at room temperature. The primary antibody solution was then discarded and the blot was extensively washed in Tween-TBS. Anti-chicken (PsbA and RbcL) or anti-rabbit (PsaC, Lhca2, and Lhcp) secondary antibodies coupled with horseradish peroxidase (Biorad) were diluted at 1 : 50,000 in Tween-TBS buffer containing

2% blocking agent, and the membrane was incubated as described above for 1 h, followed by a sequence of washing in Tween-TBS buffer. After 5 min incubation in Enhanced Chemiluminescent Reagent (ECL) Advance reagent (Amersham Biosciences) in darkness, the membrane was placed under two plastic transparent sheets and developed within an ultra sensitive imager (FluorSMax, Biorad).

Chemoluminescence signals were measured using the Quantity One software (Biorad). Protein standard curves were generated by fitting a two-factor polynomial function, and the protein concentrations were determined by fitting the sample signal values on the standard curve. Pilot experiments were performed to ensure that sample signals fell within the range spanned by the standard curve for each protein immunoquantitation.

The physical sizes of the photosynthetic antenna of PSII and PSI were estimated by calculating Lhcp to PsbA and Lhca2 to PsaC ratios, expressed as percentage of the values for *O. tauri* grown under 15 μmol photons m^{-2} s^{-1}.

Comparative resource allocations to photosystems and antenna complexes—We used the *O. tauri* genomic sequence information (Van de Peer 2005; Derelle et al. 2006) and published structures for PSI (Jordan et al. 2001), PSII (Zouni et al. 2001), and associated LHCI and LHCII antenna complexes (Nield et al. 2004) to estimate the amino acid composition for these complexes in *O.* sp. RCC809 and *O. tauri*. We used PsbA per cell as an estimate of PSII content, and multiplied by an estimate of amino acids per PSII. We similarly used PsaC per cell as an estimate of PSI content, multiplied by an estimate of amino acids per PSI.

We estimated the amino acid content per Chl *b* in the PSII and PSI antenna of *Ostreococcus*, assuming that antenna differences between the strains arise through different antenna sizes, reflected by a difference in Chl *b* content per photosystem and that the average amino acid compositions of the antenna were comparable in *O.* sp. RCC809 and in *O. tauri*. We then used the Chl *b*–per-cell data as an estimate of antenna content and multiplied by our estimate of amino acid per Chl *b* to estimate the cellular allocation of amino acids relative to antenna function in each strain. The antenna estimates were weighted to account for the PSI : PSII ratio since the compositions of the antenna associated with each photosystem were different. We then summed these amino acid allocation estimates for each strain and plotted them versus growth light.

CHN analyses—Aliquots of culture containing a known number of cells were filtered through Millipore Glass Fiber Filters, precombusted for 5 h at 400°C in order to remove any trace of organic matter. The filters were then desiccated for several days in a desiccating air-proof chamber (BelArt). Each filter was cut in half and loaded on a 96-well microplate. Caution was taken to avoid any contamination during the sample manipulations. Nitrogen concentrations were determined at the Institute of Marine and Coastal Sciences (IMCS) at Rutgers University using an elemental analyzer (Carl Erba) after calibration with standards. Values were corrected using blanks consisting of filters soaked with culture medium.

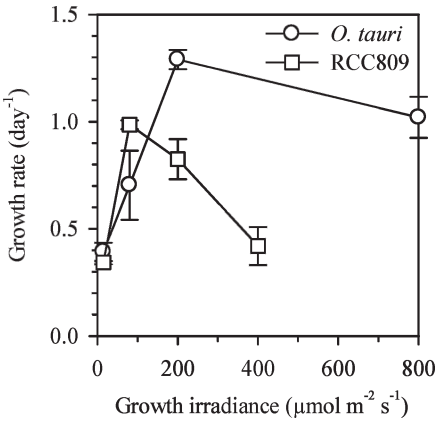

Fig. 1. Growth rates of *O. tauri* (circles) and *O.* sp. RCC809 (squares) grown under different irradiances.

Results

Growth rate variations with growth irradiance—We were able to grow the deep-sea *O.* sp. RCC809 only up to 400 μmol photons m^{-2} s^{-1} whereas the lagoon *O. tauri* could be acclimated up to at least 800 μmol photons m^{-2} s^{-1} (Fig. 1). Both *O.* sp. RCC809 and *O. tauri* had a growth rate of ~0.4 d^{-1} under 15 μmol photons m^{-2} s^{-1}. A maximal growth rate of 1.0 d^{-1} was achieved at 80 μmol photons m^{-2} s^{-1} for the deep-sea strain *O.* sp. RCC809 while the lagoon strain *O. tauri* achieved a maximal rate of 1.3 d^{-1} at 200 μmol photons m^{-2} s^{-1}. One notable particularity of *O. tauri* was that it could withstand one-step light shifts from 15 μmol photons m^{-2} s^{-1} to 800 μmol photons m^{-2} s^{-1} whereas *O.* sp. RCC809 needed progressive up scaling of growth irradiance to survive at only 400 μmol photons m^{-2} s^{-1}.

Pigment content variations between strains with growth irradiance—Chlorophyll cell content decreased with increasing growth irradiance in both *Ostreococcus* strains (Fig. 2A,B). When grown under low light, the deep-sea strain *O.* sp. RCC809 contained about 20 fg Chl *a* $cell^{-1}$ compared to 40 fg Chl *a* $cell^{-1}$ for the lagoon strain *O. tauri*, while both strains contained about 20 fg Chl *b* $cell^{-1}$. Hence, with increasing light, the Chl *b* : Chl *a* molar ratio decreased sharply from 1.03 to 0.14 in *O.* sp. RCC809, but only from 0.52 to 0.31 in *O. tauri*.

Both *Ostreococcus* strains showed a set of carotenoids characteristic for the order Mamiellales (Egeland et al. 1997; Latasa et al. 2004; Rodríguez et al. 2005) which changed with growth irradiance (Fig. 3). Both strains showed similar molar ratios to Chl *a* of neoxanthin, prasinoxanthin, micromonal, and Mg-divinyl phaeoporphyrin a_5 (MgDVP). Relative to Chl *a*, the deep-sea *O.* sp. RCC809 contained more uriolide, dihydrolutein unknown carotenoid, and α-carotene than the lagoon *O. tauri* (Fig. 3). In contrast, *O.* sp. RCC809 contained less β-carotene than *O. tauri*, especially under low growth irradiance. In both strains, the major carotenoids neoxanthin and prasinoxanthin showed only a slight decrease with increasing growth irradiance (Fig. 3A) while dihydro-

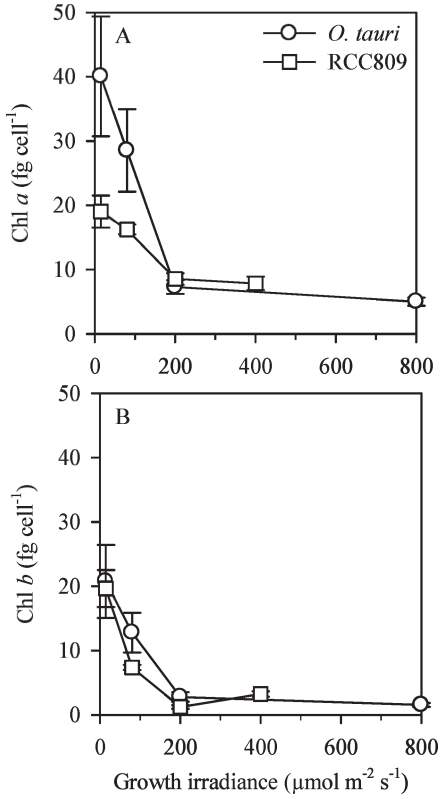

Fig. 2. (A) Chl *a* and (B) Chl *b* cell contents in *O. tauri* (circles) and *O.* sp. RCC809 (squares) grown under different irradiances.

lutein decreased in *O.* sp. RCC809 (Fig. 3D). Uriolide, the unknown carotenoid, MgDVP, and micromonal sharply decreased with increasing growth irradiance, as did the Chl CS-170 present only in the deep-sea *O.* sp. RCC809 strain (Fig. 3B, C).

In contrast, β-carotene content relative to Chl *a* increased significantly with increasing growth light (Fig. 3E). It is noteworthy that high growth irradiance also induced a strong lutein accumulation relative to Chl *a* (Fig. 3D) in cells acclimated above their optimal irradiance for growth, that is 80 μmol photons m^{-2} s^{-1} for the deep-sea *O.* sp. RCC809 and 200 μmol photons m^{-2} s^{-1} for the lagoon *O. tauri*. The DES of the xanthophyll cycle increased with growth irradiance in both strains (Fig. 3F), reflecting increasing activation of the xanthophyll cycle, particularly in the deep-sea *O.* sp. RCC809.

Photosynthetic parameter variations with growth irradiance—NPQ is an index of dissipation of excess light energy as heat. Both strains induced NPQ when measured at their growth irradiance, with sustained NPQ values of 1.1 when grown under high light (Fig. 4). When submitted to irradiances of 1,000–1,500 μmol photons m^{-2} s^{-1} for 2 min, high-light cultures of both strains could develop maximum NPQ of 2.5. NPQ correlated well with the DES of the cells (Fig. 4; $r^2 = 0.87$ for both strains included in the correlation). However, the data seemed to indicate different dynamics, with a pseudoexponential relation for *O.* sp. RCC809 and a rather linear one for *O. tauri* (Fig. 4).

Maximal PSII quantum yield ($F_V : F_M$) in the deep-sea strain *O.* sp. RCC809 remained steady across the range of

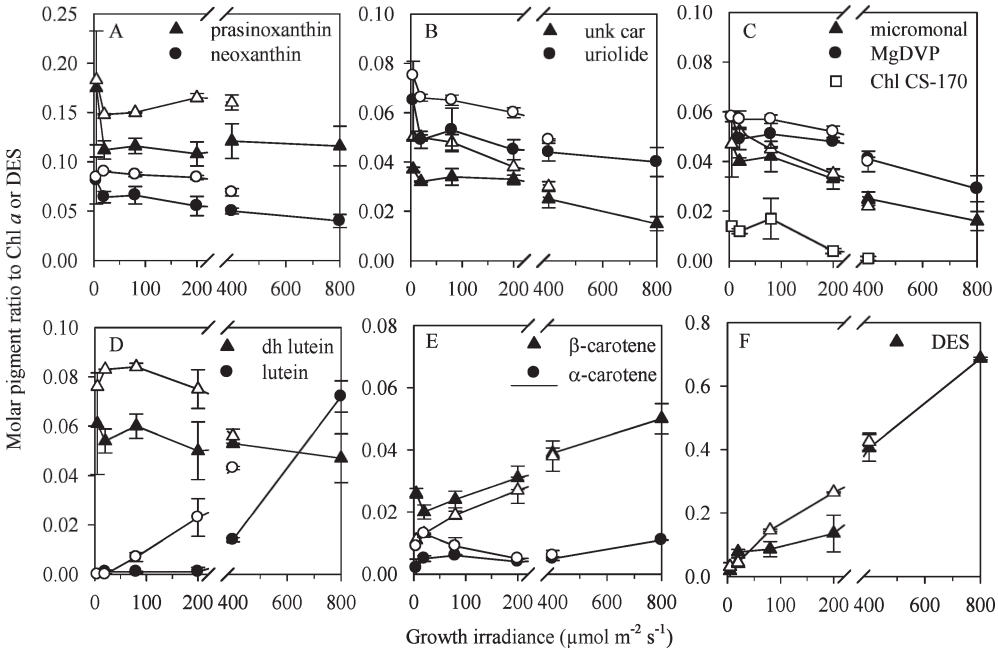

Fig. 3. Pigment analysis of *O. tauri* (closed symbols) and *O.* sp. RCC809 (open symbols) grown under different irradiances. All pigment levels are presented as molar ratios to Chl *a*. The pigmentation of *Ostreococcus* includes (A) prasinoxanthin and neoxanthin, (B) uriolide and an unknown carotenoid (unk car), (C) micromonal, MgDVP, and chlorophyll CS-170 (only present in *O.* sp. RCC809), (D) dh Lutein and lutein,(E) β- and α-carotenes and (F) DES of the xanthophyll cycle including violaxanthin, antheraxanthin, and zeaxanthin.

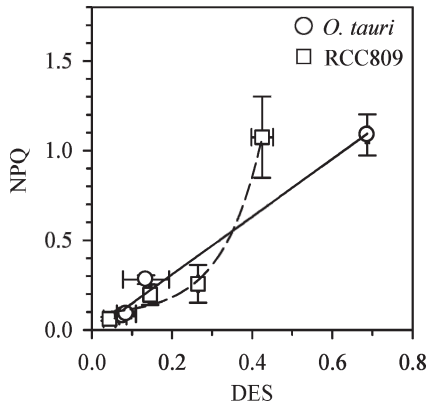

Fig. 4. NPQ plotted versus DESs of the xanthophyll cycle measured at growth irradiance in *O. tauri* (circles) and *O.* sp. RCC809 (squares) grown under different growth irradiances.

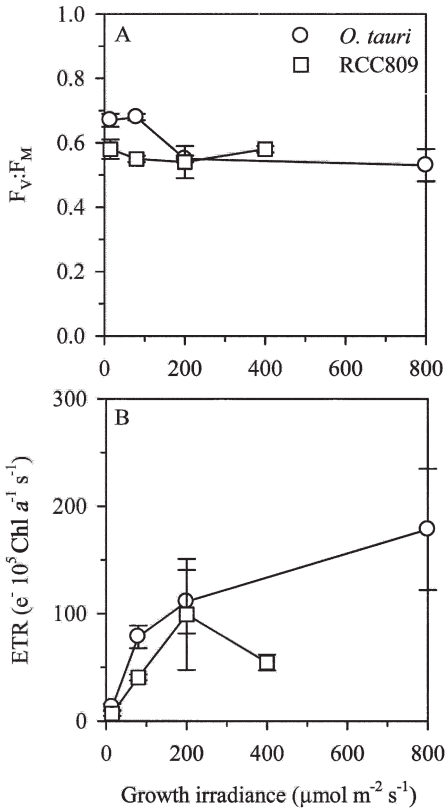

Fig. 5. (A) Maximum PSII quantum yield measured in the dark (A) and (B) electron transport rate measured at the respective growth irradiances in *O. tauri* (circles) and *O.* sp. RCC809 (squares) grown under different irradiances.

growth irradiance (Fig. 5A), while lagoon *O. tauri* displayed a higher $F_V:F_M$ when grown under low light. On a Chl *a* basis, the achieved electron transport rate, measured at growth irradiance, reached a peak in deep-sea *O.* sp. RCC809 when grown under 200 μmol photons m^{-2} s^{-1} but increased with increasing growth irradiance in *O. tauri* (Fig. 5B). The patterns of achieved electron transport rate per Chl *a* versus growth irradiance (Fig. 5B) were close but not identical to those of growth rate (Fig. 1) for each strain. In the deep-sea strain *O.* sp. RCC809, achieved electron transport on a per cell basis was similar to the per Chl *a* pattern, peaking at $9.5 \times 10^6 \pm 5.8 \times 10^6$ e^- $cell^{-1}$ s^{-1} ($n = 4$, ±SD) at 200 μmol photons m^{-2} s^{-1}. In contrast, for *O. tauri* there was no significant variation in achieved electron transport per cell ($8.2 \times 10^6 \pm 4.9 \times 10^6$ e^- $cell^{-1}$ s^{-1}; $n = 16$, ±SD) across the entire range of growth irradiances. These distinctions between the strains arose from the smaller changes in cellular Chl *a* content in *O.* sp. RCC809 compared to the large decline in Chl *a* content in *O. tauri* (Fig. 2A) with increasing growth irradiance.

Variations of photosynthetic protein complexes with growth irradiance—We quantified the growth-irradiance–induced variation in the cell content of key photosynthetic proteins PsbA, PsaC, and RbcL, reflecting the cell contents of PSII, PSI, and RuBisCO complexes, respectively. In addition, we measured relative changes in the main PSII photosynthetic antenna protein Lhcp and the LHCI protein Lhca2 associated with PSI. In the deep-sea *O.* sp. RCC809, PsbA decreased slightly with increasing growth irradiance, but PsaC cell content dropped by 70% (Fig. 6A,B). The lagoon *O. tauri* contained more PsbA and PsaC per cell across all growth irradiances, and the contents of both PsbA and PsaC sharply decreased by 80% from a growth irradiance of 15–800 μmol photons m^{-2} s^{-1} (Fig. 6A,B). The molar PsaC : PsbA reflecting the PSI to PSII ratio therefore did not significantly vary in *O. tauri* with an average value of 2.0 ± 0.5. In *O.* sp. RCC809, this ratio decreased from 3.0 ± 1.8 to 1.7 ± 1.0 from a growth irradiance of 15–400 μmol photons m^{-2} s^{-1}.

The Lhcp : PsbA ratio showed that, under low light, *O.* sp. RCC809 possessed a larger PSII antenna than *O. tauri*. The *O.* sp. RCC809 PSII antenna size, however, decreased sharply with increasing growth light (Fig. 6C) while in *O. tauri*, Lhcp : PsbA did not vary with growth light, suggesting no variation in the PSII antenna size. Lhca2 to PsaC ratio did not vary significantly in either strain, suggesting no major change in the size of the PSI antenna size in response to increasing growth irradiance (Fig. 6D).

Although some variability was observed among the replicates, the RbcL cell content was similar in both strains and did not vary with increasing growth light, with *O.* sp. RCC809 at $3.9 \times 10^5 \pm 1.2 \times 10^5$ RbcL $cell^{-1}$, and *O. tauri* at $4.4 \times 10^5 \pm 1.8 \times 10^5$ RbcL $cell^{-1}$.

Variations in photosystem II absorption cross-section—When grown under 15 μmol photons m^{-2} s^{-1}, the deep-sea *O.* sp. RCC809 displayed a large σ_{PSII} of about 6 nm^2 $PSII^{-1}$, in accordance with the large physical content of LHCII protein per reaction center (Fig. 5C), while the lagoon *O. tauri* had a σ_{PSII} of about 4 nm^2 $PSII^{-1}$ (Fig. 7A). In addition, σ_{PSII} decreased to about 3 nm^2 $PSII^{-1}$ in both strains when grown under high light (400 μmol photons m^{-2} s^{-1} or 800 μmol photons m^{-2} s^{-1}). In contrast, when grown under low light, deep-sea *O.* sp. RCC809 displayed a smaller cellular absorption cross-section for $\sigma_{PSIIcell}$ of 0.2 μm^2 $cell^{-1}$ compared to

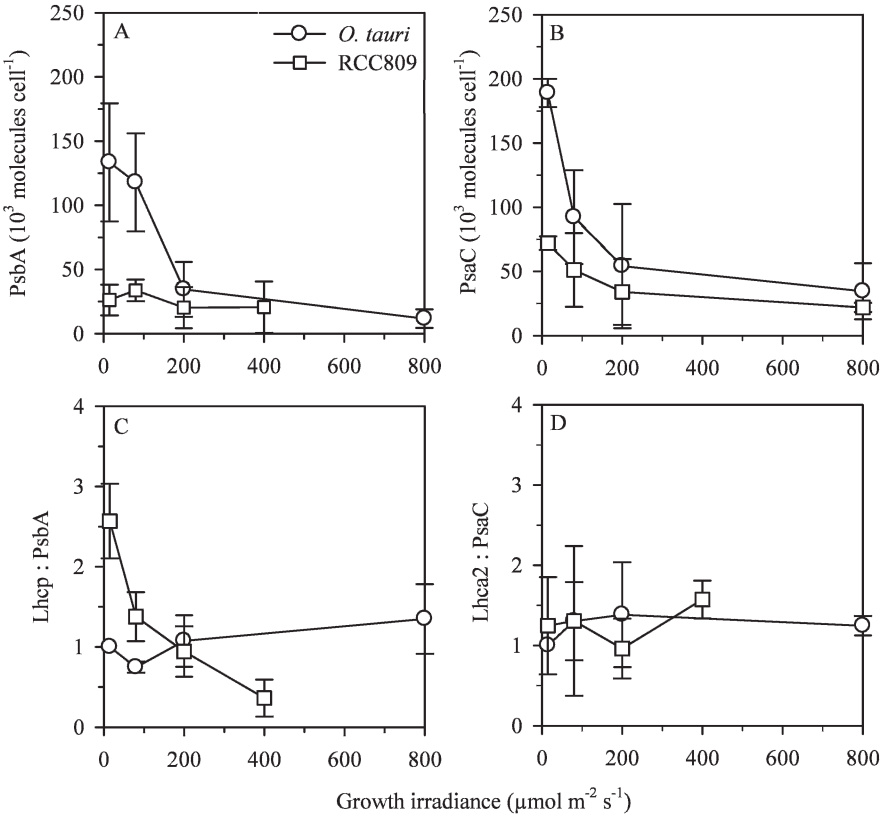

Fig. 6. (A) Variation in PsbA, (B) PsaC, (C) PSII antenna size (Lhcp : PsbA), and (D) partial PSI antenna size (Lhca2 : PsaC) in *O. tauri* (circles) and *O.* sp. RCC809 (squares) grown under different irradiances.

0.5 μm^2 $cell^{-1}$ for *O. tauri*, due to the lower PSII content in *O.* sp. RCC809 (Fig. 7B). Accordingly, $\sigma_{PSIIcell}$ decreased with increasing growth irradiance to a similar level of about 0.03 μm^2 $cell^{-1}$ in both strains grown under high light.

Comparative resource allocations to photosystems and antenna complexes and nitrogen content—O. tauri clearly incurred a higher amino acid expense for photosystems and associated antenna in order to grow under low light compared to *O.* sp. RCC809 (Fig. 8A). Under 15 μmol photons m^{-2} s^{-1}, *O. tauri* contained about three fold more amino acids associated with the photosystems than did *O.* sp. RCC809. Under low-growth irradiance, *O. tauri* likewise contained significantly more nitrogen per cell than *O.* sp. RCC809 (Fig. 8B). The C : N ratio was similar in both strains (4.9 $\pm$ 0.2) and did not vary in response to growth irradiance. These allocation differences were specific to low irradiances, decreased with increasing growth irradiances, and were negligible at 200 μmol photons m^{-2} s^{-1}.

Discussion

We investigated photosynthetic acclimation in response to growth irradiance in two prasinophyte *Ostreococcus* strains isolated from two contrasting marine environments. *O. tauri* was isolated from the shallow (4-m mean depth) and eutrophic Thau lagoon in the South of France, where this species has to cope with high irradiance and fluctuating light (Fouilland et al. 2004; Lazure 1992). In contrast, *O.* sp. RCC809 was isolated from the deep chlorophyll maximum (105 m depth) at station OLIGO in the tropical Atlantic Ocean (*see* figs. 4A and 7 in Partensky et al. 1996), where the environmental conditions are more stable and nutrients and irradiance are lower. In agreement with Rodríguez et al. (2005), our results showed that the lagoon strain *O. tauri* and the deep-sea *O.* sp. RCC809 display different growth-light responses including distinct optimal irradiances for growth and differential resistance to high growth irradiance. Indeed, the lagoon strain *O. tauri* was still able to divide once per day at 800 μmol photons m^{-2} s^{-1} while the deep-sea *O.* sp. RCC809 reached maximum growth rate at only 80 μmol photons m^{-2} s^{-1}. These two strains, although phylogenetically close (Guillou et al. 2004), exhibited different photophysiological responses even when grown under the same culture conditions, indicating that they have adapted to their respective ecological niches.

Contrasting reaction centre and antenna content between the two Ostreococcus *ecotypes*—When the two strains were both grown under low light, the lagoon strain *O. tauri* maintained a higher Chl *a* per cell than the deep-sea strain *O.* sp. RCC809, with both strains having similar Chl *b* cell content. Moreover, the content of many other accessory

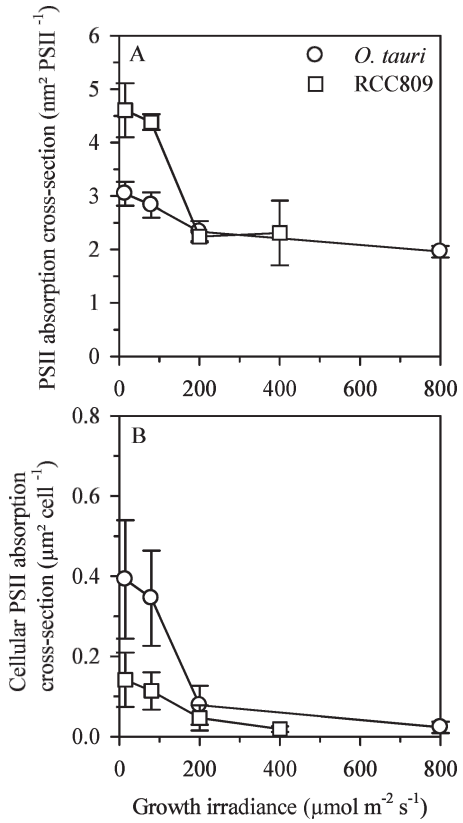

Fig. 7. (A) Variation in PSII absorption cross-section and (B) cellular PSII absorption cross-section in *O. tauri* (circles) and *O.* sp. RCC809 (squares) grown under different irradiances.

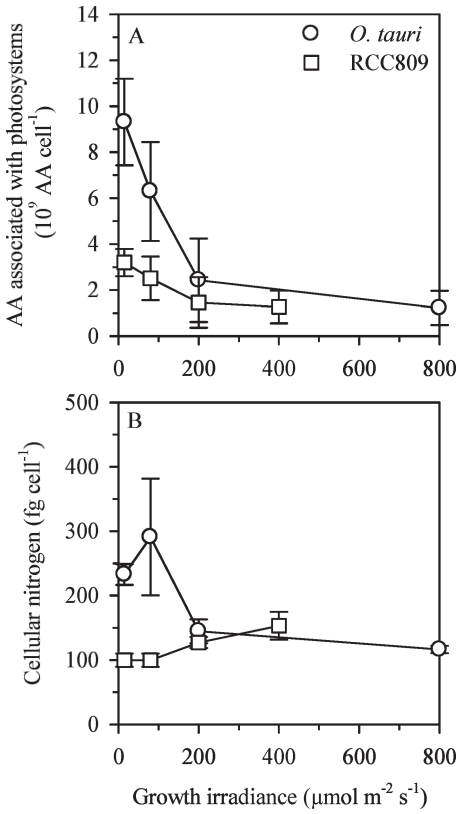

Fig. 8. (A) Cellular photosystem amino acid content as estimated using genomic information of *O. tauri* genome and published structures of reaction centers and antenna system organization and (B) nitrogen cell content in *O. tauri* (circles) and *O.* sp. RCC809 (squares) grown under different irradiances.

pigments relative to Chl *a* were lower in the lagoon *O. tauri* than in the deep-sea *O.* sp. RCC809. These differences in pigment content were largely explained by the protein quantitation data. When grown under low light, *O. tauri* showed a higher content of indicator subunits for both PSI and II than did *O.* sp. RCC809, accounting for the higher Chl *a* content of the lagoon strain. In contrast, under low-growth irradiance the ratio of PSII antenna to PSII reaction centers, indicated by Lhcp : PsbA, was about 2.5 times lower in the lagoon strain than in the deep-sea strain. Taken together, these results show that, when grown under low irradiance, the lagoon strain *O. tauri* contains more of the two photosystems, but with a proportionally smaller PSII antenna than the deep-sea strain *O.* sp. RCC809. The ratio Lhca2 : PsaC was similar in both strains and did not seem to be affected by growth irradiance, although we cannot exclude some rearrangements of the PSI antenna. Indeed, the PSI external antenna is composed of five Lhca proteins (Six et al. 2005) and we measured only the Lhca2 : PsaC ratio, because all other available anti-Lhca antibodies were incompatible with *Ostreococcus*.

The biochemical results were supported by biophysical measurements. Under low-growth irradiance, PSII centers in the lagoon strain *O. tauri* had a lower capacity for photon capture than the PSII in deep-sea *O.* sp. RCC809. Nevertheless, when the absorption cross-sections serving PSII were calculated on a per-cell basis, *O. tauri*, with a high PSII content per cell, maintained a higher overall ability to harvest photons and transfer them to the PSII reaction centers than did *O.* sp. RCC809. Nevertheless, under low light *O.* sp. RCC809 maintained growth rates comparable to *O. tauri*, suggesting that *O. tauri* incurs a higher electron cost for growth.

Light dissipation through a xanthophyll cycle and lutein accumulation in Ostreococcus?—When comparing two strains from such contrasting light environments, one might expect differences in the induction of photoprotective mechanisms such as NPQ. Both *Ostreococcus* strains, however, induce fairly strong NPQ when grown under high light, as observed previously in the Prasinophyceae *Mantoniella squamata* (Juneau and Harrison 2005), another member of the primitive Prasinophyceae family. As expected, the *O. tauri* genome expresses the genes encoding the PsbS and xanthophyll de-epoxidase proteins required for induction of high energy NPQ in land plants (Li et al. 2000). *Ostreococcus* shows xanthophyll cycle function (Demmig-Adams and Adams 1992) with DES values (e.g., Kurasova et al. 2002; Munne-Bosch and Cela 2006), that correlate well with NPQ. The functional violaxanthin cycle in Prasinophyceae suggests that this process is evolutionarily ancient in the Chlorophyte lineage and may indeed date from the origins of the LHC-type antenna.

Interestingly, both *Ostreococcus* strains accumulated lutein only at irradiances higher than the optimum for growth. Lutein was not detectable in the low-light *Ostreococcus* cultures. Thus, as in higher plants, it is not essential for photosynthesis (Pogson et al. 1996), but rather likely acts as a photoprotective pigment (Niyogi et al. 1997; Horton and Ruban 2005). We did not, however, detect any obvious break point in the NPQ induction at the optimal-growth irradiance that would correspond to a lutein-mediated phase of NPQ. In some higher plants, a lutein–lutein epoxide cycle works in parallel with the violaxanthin cycle (Garcia- Plazaola et al. 2003; Matsubara et al. 2005), but no lutein-epoxide was detected in *Ostreococcus*.

Costs and benefits of n- and σ-type photoacclimation in Ostreococcus *spp.*—Falkowski and Owens (1980) showed that the chlorophyte *Dunaliella tertiolecta* was able to withstand high-growth irradiance through changes in the number of reaction centers, a strategy termed n-type photoacclimation. In contrast, the diatom *Skeletonema costatum*, which grew optimally under lower light, responded to decreasing growth irradiance through an increase of the antenna absorption cross-section serving reaction center, a strategy termed σ-type photoacclimation.

The lagoon ecotype *O. tauri* has evolved to use n-type photoacclimation by increasing the number of PSII units with decreasing growth irradiance. In contrast, the deep-sea *O.* sp. RCC809 exhibits σ-type photoacclimation by increasing the size of the light harvesting antennae and thus the absorption cross-section for each PSII with decreasing irradiance. It is noteworthy that *D. tertiolecta* and *O. tauri*, which have evolved n-type photoacclimation, are able to cope with sustained high-growth irradiances whereas *S. costatum* and *O.* sp. RCC809, which have evolved σ-type photoacclimation, cannot. This supports Behrenfeld et al. (1998) who suggested that a large cellular pool of PSII is advantageous for coping with variable high light (Kana et al. 2002). In comparison, modifying the cross-section of PSIIs by modulating the antenna size, in σ-type photoacclimation, may exacerbate the susceptibility of reaction center II to photodamage. Thus, environments where irradiance is variable and often reaches high levels, such as the upper mixed layers of lagoons and open ocean, appear to have favoured phytoplankton genotypes capable of large modulations of photosystem content, with little change in the antenna size. In contrast, stable environments characterized by lower irradiance such as the deep chlorophyll maximum, a commonly observed feature in oligotrophic regions of the open ocean, may select organisms with fewer photosystems equipped with an antenna with of a variable size. It is possible that a large membrane antenna encumbers the rate and extent of the PSII repair cycle, thereby excluding the σ-type photoacclimation ecotypes from exploiting the more dynamic, higher-nutrient, coastal niches exploited by n-type photoacclimation ecotypes.

The n-type photoacclimation then appears to be a generalist strategy that enables the ecotype to exploit a large range of irradiances. In contrast, the σ-type photoacclimation is more specialized and confines the ecotype *O.* sp. RCC809 to a lower, narrower range of irradiances. In addition, when grown under nutrient repletion, *O.* sp. RCC809 exhibits little or no increase in growth rate over *O. tauri* even under low irradiances. The σ-type photoacclimation is, however, a lower-cost strategy, requiring a lower cellular allocation of amino acids, and thus nitrogen, to photosystems. To exploit the shifting and relatively high irradiances of the Thau lagoon in the south of France, *O. tauri* requires a high turnover of photosystem complexes with numerous subunits, pigments, and associated cofactors such as iron. This photosynthetic plasticity requires high rates of nutrient assimilation, particularly nitrogen and iron, and rapid protein synthesis that must be supported by electron transport and carbon fixation. In the nutrient-rich Thau lagoon, *O. tauri* has the resources necessary for n-type photoacclimation. If nutrients are lower and the irradiance range is narrow, changing synthesis of antenna complexes is an adequate, relatively low-cost strategy. The σ-type specialist strategy of *O.* sp. RCC809 allows the ecotype to exploit an ecological niche with a lower concentration of nutrients available from above the nutricline typically at the base of the deep chlorophyll maximum (e.g., Partensky et al. 1996), and where solar energy varies little, and the generation of photochemical electrons likely limits growth. Similarly, Strzepek and Harrison (2004) described sister diatom taxa which have evolved contrasting compositions of photosynthetic complexes to accommodate and exploit distinct nutrient selection regimes. Genomic sequences of *O. tauri* and the Pacific Ocean surface strain *Ostreococcus lucimarinus* are already available (Derelle et al. 2006; Palenik et al. 2007) and the one of *O.* sp. RCC809 will soon be available. The comparison of these three *Ostreococcus* genomes will provide new insights in the ecotypic differentiation phenomenon in this primitive and ecologically important green alga group.

Ostreococcus is a widespread genus and can be locally abundant in the marine environment (Worden et al. 2004; Countway and Caron 2006; Fuller et al. 2006), with distinct photophysiological ecotypes exploiting contrasting niches. The flexible photosynthetic antenna of the deep-sea strain *O.* sp. RCC809 could be a consequence of *lhcp* gene duplications and diversification, similar to the *pcb* genes of the low-light–adapted *Prochlorococcus* strains (Bibby et al. 2003). Modulation of the photosynthetic antenna is a low-cost strategy to exploit low-light niches, but this σ-type photoacclimation correlates with susceptibility to photoinhibition under variable or higher light. In contrast, n-type photoacclimation through dynamic regulation of photosystem content accommodates exploitation of a wider range of light, but carries a heavy nutrient cost for low-light growth.

References

Anderson, T. R. 2005. Plankton functional type modelling: Running before we can walk? J. Plankton Res. **27:** 1073–1081.

Behrenfeld, M. J., O. Prasil, Z. S. Kolber, M. Babin, and P. G. Falkowski. 1998. Compensatory changes in Photosystem II electron turnover rates protect photosynthesis from photoinhibition. Photosynth. Res. **58:** 259–268.

Bibby, T. S., I. Mary, J. Nield, F. Partensky, and J. Barber. 2003. Low-light–adapted *Prochlorococcus* species possess specific antennae for each photosystem. Nature **424:** 1051–1054.

Chrétiennot-Dinet, M. J., C. Courties, A. Vaquer, J. Neveux, H. Claustre, J. Lautier, and M. C. Machado. 1995. A new marine picoeucaryote: *Ostreococcus tauri* gen et sp. nov. (Chlorophyta, Prasinophyceae). Phycologia **34:** 285–292.

Countway, P. D., and D. A. Caron. 2006. Abundance and distribution of *Ostreococcus* sp. in the San Pedro Channel, California, as revealed by quantitative PCR. Appl. Environ. Microbiol. **72:** 2496–2506.

Demmig-Adams, B., and W. W. Adams. 1992. Photoprotection and other responses of plants to high light stress. Annu. Rev. Plant Physiol. Plant Mol. Biol. **7:** 1–116.

Derelle, E., and others. 2006. Genome analysis of the smallest free-living eukaryote *Ostreococcus tauri* unveils many unique features. Proc. Natl. Acad. Sci. USA **103:** 11647–11642.

Egeland, E. S., R. R. L. Guillard, and S. LiaaenJensen. 1997. Algal carotenoids. 63. Carotenoids from Prasinophyceae. 7. Additional carotenoid prototype representatives and a general chemosystematic evaluation of carotenoids in Prasinophyceae (Chlorophyta). Phytochemistry **44:** 1087–1097.

Falkowski, P. G., and J. A. Raven. 1997. Aquatic photosynthesis. Blackwell Science.

———, and T. G. Owens. 1980. Light-shade adaptation—two strategies in marine phytoplankton. Plant Physiol **66:** 592–595.

Fouilland, E., C. Descolas-Gros, C. Courties, Y. Collos, A. Vaquer, and A. Gasc. 2004. Productivity and growth of a natural population of the smallest free-living eukaryote under nitrogen deficiency and sufficiency. Microb. Ecol. **48:** 103–110.

Fuller, N. J., and others. 2006. Analysis of photosynthetic picoeukaryotic diversity at open ocean sites in the Arabian Sea using a PCR biased towards marine algal plastids. Aquat. Microb. Ecol. **43:** 79–93.

Garcia-Plazaola, J. I., A. Hernandez, J. M. Olano, and J. M. Becerril. 2003. The operation of the lutein-epoxide cycle correlates with energy dissipation. Funct. Plant Biol. **31:** 815–823.

Gorbunov, M. Y., Z. S. Kolber, and P. G. Falkowski. 1999. Measuring photosynthetic parameters in individual algal cells by Fast Repetition Rate fluorometry. Photosynth. Res. **62:** 141–153.

Goss, R. 2003. Substrate specificity of the violaxanthin de-epoxidase of the primitive green alga *Mantoniella squamata* (Prasinophyceae). Planta **217:** 801–812.

Gregg, W. W., P. Ginoux, P. S. Schopf, and N. W. Casey. 2003. Phytoplankton and iron: Validation of a global three-dimension ocean biogeochemical model. Deep-Sea Res. Part II **50:** 3143–3169.

Guillou, L., and others. 2004. Diversity of picoplanktonic prasinophytes assessed by direct nuclear SSU rDNA sequencing of environmental samples and novel isolates retrieved from oceanic and coastal marine ecosystems. Protist **155:** 193–214.

Horton, P., and A. Ruban. 2005. Molecular design of the photosystem II light-harvesting antenna: Photosynthesis and photoprotection. J. Exp. Bot. **56:** 365–373.

Jeffrey, S. W., R. F. C. Mantoura, and S. W. Wright. 1997. Phytoplankton pigments in oceanography. UNESCO.

Jordan, P., P. Fromme, H. T. Witt, O. Klukas, W. Saenger, and N. Krauss. 2001. Three-dimensional structure of cyanobacterial photosystem I at 2.5 angstrom resolution. Nature **411:** 909–917.

Juneau, P., and P. J. Harrison. 2005. Comparison by PAM fluorometry of photosynthetic activity of nine marine phytoplankton grown under identical conditions. Photochem. Photobiol. **81:** 649–653.

Kana, R., D. Lazar, O. Prasil, and J. Naus. 2002. Experimental and theoretical studies on the excess capacity of Photosystem II. Photosynth. Res. **72:** 271–284.

Keller, M. D., R. C. Selvin, W. Claus, and R. R. L. Guillard. 1987. Media for the culture of oceanic ultraphytoplankton. J. Phycol. **23:** 633–638.

Kurasova, I., M. Cajanek, J. Kalina, O. Urban, and V. Spunda. 2002. Characterization of acclimation of *Hordeum vulgare* to high irradiation based on different responses of photosynthetic activity and pigment composition. Photosynth. Res. **72:** 71–83.

Latasa, M., R. Scharek, F. Le Gall, and L. Guillou. 2004. Pigment suites and taxonomic groups in Prasinophyceae. J. Phycol. **40:** 1149–1155.

Lazure, P. 1992. Etude de la dynamique de l'étang de Thau par modèle tridimentionnel. Vie et Milieu **42:** 137–145.

Li, X. P., O. Björkman, C. Shih, A. R. Grossman, M. Rosenquist, S. Jansson, and K. K. Niyogi. 2000. A pigment-binding protein essential for regulation of photosynthetic light harvesting. Nature **403:** 391–395.

Mackenzie, T. D., J. M. Johnson, and D. A. Campbell. 2005. Dynamics of fluxes through photosynthetic complexes in response to changing light and inorganic carbon acclimation in *Synechococcus elongatus*. Photosynth. Res. **85:** 341–357.

Matsubara, S., and others. 2005. Slowly reversible de-epoxidation of lutein-epoxide in deep shade leaves of a tropical tree legume may 'lock-in' lutein-based photoprotection during acclimation to strong light. J. Exp. Bot. **56:** 461–468.

Moore, L. R., R. Goericke, and S. W. Chisholm. 1995. Comparative physiology of *Synechococcus* and *Prochlorococcus*: Influence of light and temperature on growth, pigments, fluorescence, and absorptive properties. Mar. Ecol. Prog. Ser. **116:** 259–275.

———, A. F. Post, G. Rocap, and S. W. Chisholm. 2002. Utilization of different nitrogen sources by the marine cyanobacteria *Prochlorococcu*s and *Synechococcus*. Limnol. Oceanogr. **47:** 989–996.

Munne-Bosch, S., and J. Cela. 2006. Effects of water deficit on photosystem II photochemistry and photoprotection during acclimation of lyreleaf sage (*Salvia lyrata* L.) plants to high light. J. Photochem. Photobiol. B **85:** 191–197.

Nield, J., K. Redding, and M. Hippler. 2004. Remodeling of light-harvesting protein complexes in *Chlamydomonas* in response to environmental changes. Eukaryot. Cell **3:** 1370–1380.

Niyogi, K. K., O. Bjorkman, and A. R. Grossman. 1997. The roles of specific xanthophylls in photoprotection. Proc. Natl. Acad. Sci. USA **94:** 14162–14167.

Not, F., M. Latasa, D. Marie, T. Cariou, D. Vaulot, and N. Simon. 2004. A single species, *Micromonas pusilla* (Prasinophyceae), dominates the eukaryotic picoplankton in the western English Channel. Appl. Environ. Microbiol. **70:** 4064–4072.

Palenik, B., and others. 2007. The tiny eukaryote *Ostreococcus* provides genomic insights into the paradox of plankton speciation. Proc. Natl. Acad. Sci. USA **104:** 7705–7710.

Partensky, F., J. Blanchot, F. Lantoine, J. Neveux, and D. Marie. 1996. Vertical structure of picophytoplankton at different trophic sites of the tropical northeastern Atlantic Ocean. Deep-Sea Res. Part I Oceanogr. Res. Pap. **43:** 1191–1213.

———, W. R. Hess, and D. Vaulot. 1999. *Prochlorococcus*, a marine photosynthetic prokaryote of global significance. Microbiol. Mol. Biol. Rev. **63:** 106–127.

Pogson, B., K. A. McDonald, M. Truong, G. Britton, and D. Dellapenna. 1996. *Arabidopsis* carotenoid mutants demonstrate that lutein is not essential for photosynthesis in higher plants. Plant Cell **8:** 1627–1639.

Porra, R. J. 2002. The chequered history of the development and use of simultaneous equations for the accurate determination of chlorophylls *a* and *b*. Photosynth. Res. **73:** 149–156.

Repeta, D. J., and T. Bjørnland. 1997. Preparation of carotenoid standards, p. 239–260. *In* S. W. Jeffrey, R. F. C. Mantoura and S. W. Wright [eds.], Phytoplankton pigments in oceanography: Guidelines to modern methods. UNESCO.

Rodríguez, F., E. Derelle, L. Guillou, F. Le Gall, D. Vaulot, and H. Moreau. 2005. Ecotype diversity in the marine picoeukaryote *Ostreococcus* (Chlorophyta, Prasinophyceae). Environ. Microbiol. **7:** 853–859.

Six, C., J. C. Thomas, B. Brahamsha, Y. Lemoine, and F. Partensky. 2004. Photophysiology of the marine cyanobacterium *Synechococcus* sp. WH8102, a new model organism. Aquat. Microb. Ecol. **35:** 17–29.

———, A. Z. Worden, F. Rodriguez, H. Moreau, and F. Partensky. 2005. New insights into the nature and phylogeny of prasinophyte antenna proteins: *Ostreococcus tauri*, a case study. Mol. Biol. Evol. **22:** 2217–2230.

Strzepek, R. F., and P. J. Harrison. 2004. Photosynthetic architecture differs in coastal and oceanic diatoms. Nature **431:** 689–692.

Van de Peer, Y., and others. 2005. Ostreococcus tauri: Mitochondrial DNA and chloroplast DNA [Internet]. Gent, (Belgium): Flanders Institute for Biotechnology, Universiteit Gent, Department of Bioinformatics & Evolutionary Genomics; 2005 June [accessed 2007 Sep 30].Available from http://bioinformatics.psb.ugent.be/genomes/ostreococcus_tauri/

Worden, A. Z., J. K. Nolan, and B. Palenik. 2004. Assessing the dynamics and ecology of marine picophytoplankton: The importance of the eukaryotic component. Limnol. Oceanogr. **49:** 168–179.

Zouni, A., H. T. Witt, J. Kern, P. Fromme, N. Krauss, W. Saenger, and P. Orth. 2001. Crystal structure of photosystem II from *Synechococcus elongatus* at 3.8-angstrom resolution. Nature **409:** 739–743.

Received: 12 March 2007
Amended: 1 September 2007
Accepted: 13 September 2007